VIP Nanotubes Very Important Paper

Deutsche Ausgabe: DOI: 10.1002/ange.201505806
Internationale Ausgabe: DOI: 10.1002/anie.201505806

Selective Synthesis of Single- and Multi-Walled Supramolecular Nanotubes by Using Solvophobic/Solvophilic Controls: Stepwise Radial Growth via "Coil-on-Tube" Intermediates

Seelam Prasanthkumar, Wei Zhang, Wusong Jin, Takanori Fukushima,* and Takuzo Aida**

Abstract: *Novel hexa-peri-hexabenzocoronene (HBC) derivatives, ^{F}HBC and ^{F}HBC*, which carry perfluoroalkyl segments on one side of the HBC core and long alkyl tails on the other, were synthesized. Their perfluoroalkyl segments are highly solvated in C_6F_6 (solvophilic effect) and do not assemble, whereas in CH_2Cl_2, they are excluded (solvophobic effect) and assemble together consequently. For example, the use of C_6F_6 and CH_2Cl_2 as assembling media for ^{F}HBC leads to the selective formation of single- and multi-walled nanotubes, respectively. When a higher monomer concentration is applied in CH_2Cl_2, multi-walled nanotubes with a larger number of walls result. ^{F}HBC in CH_2Cl_2 self-assembles rather slowly, thereby allowing for the observation of coil-on-tube structures, which are possible intermediates for the stepwise radial growth of the nanotubular wall. Casting of the multi-walled nanotubes onto a quartz plate yields a superhydrophobic thin film with a water contact angle of 161 ± 2°.*

Because single and multi-walled carbon nanotubes have different physical properties,[1] a large number of synthetic investigations have been performed to establish a method for selectively obtaining these morphologically different nanotubes on a large scale.[2] In supramolecular chemistry and materials science, nanotubes are also of key interest, since self-assembly of small molecules into such low-symmetry hollow objects still remains a difficult issue to tackle.[3] Although nanotubes and nanofibers are categorized as one-dimensional objects, they are essentially different from one another because nanotubes are composed of rolled-up two-dimensional (2D) nanosheets. Hence, despite the fact that both single- and multi-walled supramolecular nanotubes have been reported,[4] it has been considered a big challenge to control the number of nanotubular walls by changing the self-assembling conditions.

Herein we report an approach for this elaborate structural control of nanotubes by manipulating the solvophilic/solvophobic effects on the self-assembly event. The molecular platform we chose is a Gemini-shaped amphiphilic hexa-*peri*-hexabenzocoronene (HBC) with triethylene glycol (TEG) side chains on one side of its HBC core and dodecyl tails on the other (^{TEG}HBC, Figure 1a). As reported for the first time in 2004,[5] this particular HBC molecule self-assembles into single-walled nanotubes (SWNTs) in polar solvents, such as THF. Synchrotron-radiation X-ray diffraction (XRD) analysis revealed that the nanotubular wall is composed of a helically coiled bilayer tape consisting of π-stacked HBC *J*-aggregates. The inner and outer HBC layers are connected by interdigitation of the dodecyl tails (Figure 1c),[6] whereas the polar TEG chains that cover the nanotube surface are solvated in THF and suppress further assembly that leads to the multiplication of the nanotubular wall. So, we envisioned if a HBC derivative having long alkyl chains on both sides of its HBC core (^{C12}HBC, Figure 1a) might self-assemble into multi-walled nanotubes. However, only ill-defined agglomerates formed,[6] most likely as a consequence of the HBC units not being able to differentiate between two different paraffinic chains in the self-assembly event. In the current study, we designed ^{F}HBC and ^{F}HBC* (Figure 1b), which bear, at one side of the HBC core, perfluoroalkyl segments that are incompatible[7] with the dodecyl tails attached onto the other side. As illustrated in Figure 2, the newly designed HBC derivatives, under optimized conditions, self-assemble into SWNTs in perfluorobenzene (C_6F_6) and into multi-walled nanotubes (MWNTs) in non-fluorous polar media, such as CH_2Cl_2 (for ^{F}HBC) and CH_2Cl_2/MeOH (for ^{F}HBC*). Furthermore, we successfully observed morphologically interesting "coil-on-tube" structures, which are possible intermediates for the multiplication of the nanotubular wall. This radial growth mechanism essentially differs from the precedent mechanism in which 2D nanosheets are rolled up for scrolling.[3b,d]

Perfluoroalkyl-appended HBC derivatives ^{F}HBC and ^{F}HBC* (Figure 1b) were synthesized by oxidative cyclization of the corresponding hexaphenylbenzene precursors bearing perfluoroalkyl segments; the oxidative cyclization was performed using $FeCl_3$/$MeNO_2$ in CH_2Cl_2.[8] The solubilities of ^{F}HBC and ^{F}HBC* in organic solvents differ substantially from that of our prototype, ^{TEG}HBC. In sharp contrast to ^{TEG}HBC,

[*] Dr. S. Prasanthkumar, Dr. W. Zhang, Prof. Dr. T. Aida
RIKEN Center for Emergent Matter Science
2-1 Hirosawa, Wako, Saitama 351-0198 (Japan)
E-mail: aida@macro.t.u-tokyo.ac.jp
Prof. Dr. W. Jin
State Key Laboratory for Modification of Chemical Fibers and Polymer Materials, College of Chemistry, Chemical Engineering and Biotechnology, Donghua University
2999 North Renmin Road, Songjiang, Shanghai 201620 (P. R. China)
E-mail: wsjin@dhu.edu.cn
Prof. Dr. T. Fukushima
Chemical Resources Laboratory, Tokyo Institute of Technology
4159 Nagatsuta, Midori-ku, Yokohama 226-8503 (Japan)
E-mail: fukushima@res.titec.ac.jp
Prof. Dr. T. Aida
Department of Chemistry and Biotechnology, School of Engineering, The University of Tokyo
7-3-1 Hongo, Bunkyo-ku, Tokyo 113-8656 (Japan)

Supporting information for this article is available on the WWW under http://dx.doi.org/10.1002/anie.201505806.

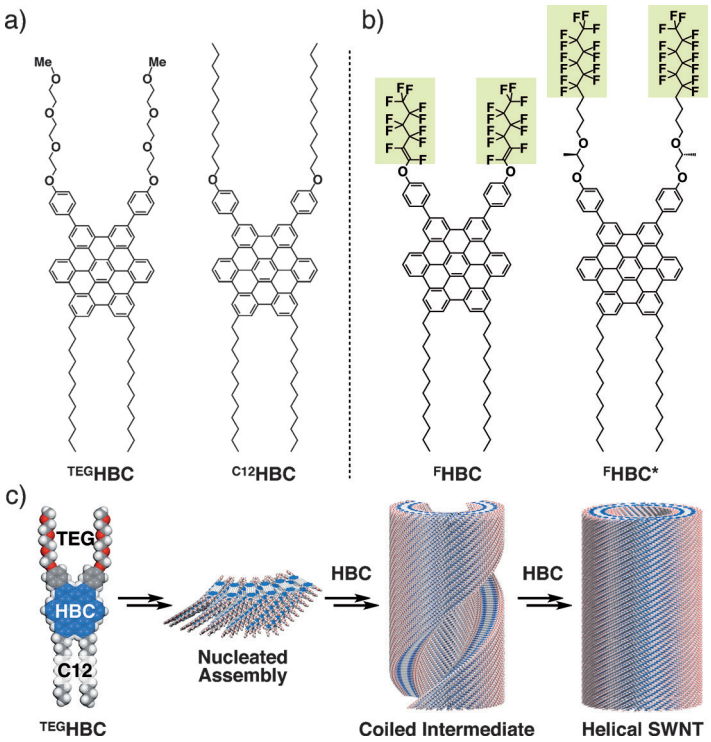

Figure 1. Structural formulas of a) ^{TEG}HBC and ^{C12}HBC, together with b) perfluoroalkyl-appended HBC derivatives ^{F}HBC and ^{F}HBC*. c) Schematic representation of the self-assembly of ^{TEG}HBC into a SWNT through a coiled intermediate of *J*-aggregated ^{TEG}HBC.

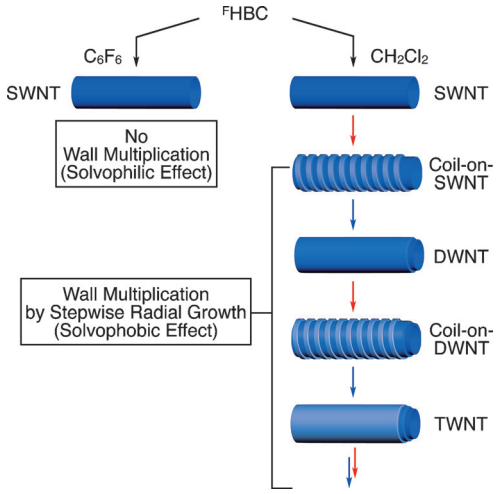

Figure 2. Schematic representations of single- and multi-walled nanotubes of ^{F}HBC assembled in C_6F_6 and CH_2Cl_2, respectively, and stepwise radial growth via coil-on-tube intermediates.

perfluoroalkyl-appended ^{F}HBC was highly soluble in THF at ambient temperatures and did not assemble. Upon being cooled from 50 to 0 °C, ^{F}HBC started to assemble but afforded an ill-defined fibrous agglomerate (Figure S2 in the Supporting Information).[8] However, after numerous trials, we found that ^{F}HBC self-assembles into nanotubes in CH_2Cl_2, whereas the prototype, ^{TEG}HBC, does not. Typically, a CH_2Cl_2 suspension of ^{F}HBC (1 mg mL^{-1}) is heated to reflux for a short time after being ultrasonicated, and the resulting transparent solution is allowed to stand at 25 °C for 24 h, whereupon a yellow substance precipitates. For electronic absorption spectroscopy, a small portion of this precipitate was dispersed in MeOH, and showed a main absorption band at 365 nm, along with red-shifted shoulders at 418 and 441 nm (Figure S3a); these shoulders are characteristic of *J*-aggregated HBC units.[5] Scanning electron microscopy (SEM) of an air-dried CH_2Cl_2 suspension of ^{F}HBC revealed nanoscale cylindrical objects with an inner hollow space (Figure 3a). High-resolution transmission electron microscopy (TEM) allowed us to count the number of nanotubular walls. For example, the TEM image in Figure 3c clearly shows a triple-walled nanotubular (TWNT) structure with outer and inner diameters of approximately 35 and 17 nm, respectively, and a wall thickness of approximately 9 nm. On the basis of the TEM images, we also confirmed the presence of double- and quadruple-walled nanotubes in addition to TWNTs in the assembling mixture (Figure S4).

In contrast, when hexafluorobenzene (C_6F_6) was used, ^{F}HBC self-assembled into SWNTs exclusively. For example, when a hot C_6F_6 solution of ^{F}HBC (1 mg mL^{-1}) was allowed to stand at 25 °C for 24 h, yellow flakes formed at the air/organic interface. The electronic absorption spectrum of this flake dispersed in MeOH was almost identical to that of MWNT (Figure S3b). SEM microscopy (Figure 3b) indicated that these flakes are bundles of unidirectionally oriented nanotubes. High-resolution TEM microscopy (Figure 3d) confirmed that these nanotubes are all single-walled with uniform outer and inner diameters of approximately 18 and 12 nm, respectively, and a wall thickness of approximately 3 nm.

FT-IR spectroscopy of a cast film of the MWNTs of ^{F}HBC showed CH_2 stretching vibration bands at 2918 (ν_{anti}) and 2848 cm^{-1} (ν_{sym}) (Figure S5a), indicating that the dodecyl tails of ^{F}HBC are stretched to form a crystalline domain.[6] Therefore, as is the case for the single-walled ^{TEG}HBC nanotube,[5] each wall in the ^{F}HBC-based MWNT adopts a bilayer geometry. An analogous FT-IR spectral profile was observed for the SWNTs of ^{F}HBC, whose CH_2 stretching vibrations appeared at 2920 (ν_{anti}) and 2850 cm^{-1} (ν_{sym}) (Figure S5b). The bilayer geometry of each wall, supported by interdigitation of the stretched dodecyl tails, indicates that the outer and inner surfaces of each wall are covered by the perfluoroalkyl segments. In fact, the contact angle of a water droplet at 21 °C on a cast film composed of the SWNTs of ^{F}HBC was 126 ± 4° (Figure 4b), which is much larger than that of our prototype ^{TEG}HBC nanotube wrapped by polar TEG chains (45.5°).[5] We also prepared a cast film of the MWNTs of ^{F}HBC. Because of an additional surface roughness effect induced by the large-diameter multi-walled nanotubular constituents, the contact angle (161 ± 2°; Figure 4a) was observed to be in a range referred to as "superhydrophobicity"[9] and much larger than that for the SWNT version described above. In the formation of multi-walled nanotubular ^{F}HBC in CH_2Cl_2, its perfluoroalkyl segments possibly

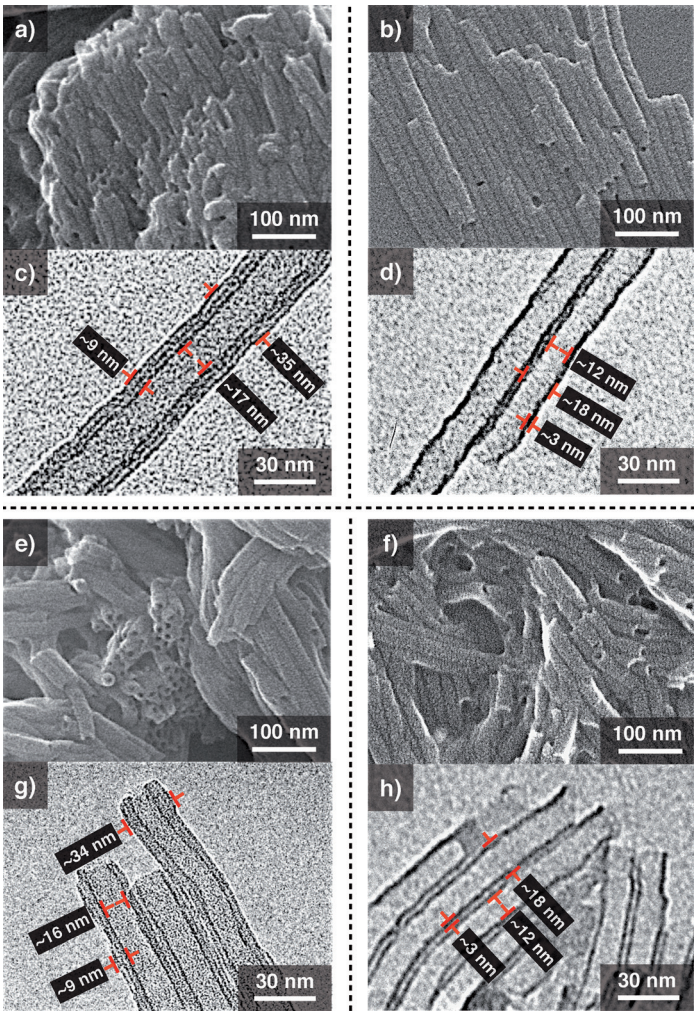

Figure 3. a,c) SEM and TEM images of an air-dried CH_2Cl_2 suspension (1 mg mL^{-1}) of ^{F}HBC kept in advance at 25 °C for 24 h. b,d) SEM and TEM images of an air-dried C_6F_6 suspension (1 mg mL^{-1}) of ^{F}HBC. e,g) SEM and TEM images of an air-dried suspension of ^{F}HBC* prepared by MeOH vapor diffusion into a CH_2Cl_2 solution of ^{F}HBC* (1 mg mL^{-1}) at 25 °C. f,h) SEM and TEM images of an air-dried suspension of ^{F}HBC* prepared by cooling its hot C_6F_6 solution (1 mg mL^{-1}) to 25 °C.

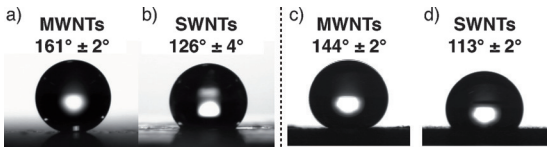

Figure 4. Pictures of water droplets on quartz plates coated with CH_2Cl_2 (a,c) and C_6F_6 (b,d) suspensions of multi- and single-walled nanotubularly assembled ^{F}HBC (a,b) and ^{F}HBC* (c,d) at 1 mg mL^{-1} in air at 21 °C with a humidity level of 27%.

behave solvophobically and play a crucial role. Accordingly, in a fluorous solvent, such as C_6F_6, this solvophilic effect is attenuated, so that a SWNT structure results.

^{F}HBC* (Figure 1b) carries a long and branched paraffinic segment between the perfluoroalkyl and HBC units. In contrast to ^{F}HBC, this HBC derivative was highly soluble in CH_2Cl_2 and did not assemble without the assistance of a poor solvent, such as MeOH. Thus, when MeOH vapor was allowed to diffuse into a CH_2Cl_2 solution of ^{F}HBC* (1 mg mL^{-1}) over a period of 12 h at 25 °C, a yellow-colored suspension formed. To prepare a dispersion, an aliquot of this suspension was transferred to MeOH. Analogous to the case of ^{F}HBC, the resulting dispersion exhibited a typical *J*-aggregate absorption spectral feature (Figure S6a). An SEM image of the air-dried suspension showed bundled nanotubes (Figure 3e). High-resolution TEM images confirmed that the nanotubes are multi-walled. For example, all three nanotubes highlighted in Figure 3g are triple-walled with outer and inner diameters of approximately 34 and 16 nm, respectively, and a wall thickness of approximately 9 nm. Closer examination of the TEM image revealed that the nanotubes partly lack outer walls or carry fragments of additional walls. Despite the presence of these structural defects, the overall size regime of the multi-walled ^{F}HBC* nanotube is virtually the same as that obtained from ^{F}HBC (Figure 3c). Similar to the case of ^{F}HBC, when a hot C_6F_6 solution of ^{F}HBC* (1 mg mL^{-1}) was allowed to cool to room temperature, this HBC derivative self-assembled exclusively into SWNTs with uniform outer and inner diameters of approximately 18 and 12 nm, respectively, and a wall thickness of approximately 3 nm (Figure 3f and h). Together with electronic absorption spectra (Figure S6), FT-IR data (Figure S7) for the multi- and single-walled ^{F}HBC* nanotubes, along with their contact angle measurements (Figure 4c and d), indicate features and trends analogous to those observed for the multi- and single-walled ^{F}HBC nanotubes, respectively. Importantly, the remarkable solvent effect on the assembly mode of ^{F}HBC* again indicates a crucial role of the perfluoroalkyl segments as solvophilic/solvophobic handles.

In CH_2Cl_2, the perfluoroalkyl segments solvophobically assemble, as described above, so that the number of walls in the nanotube tends to be larger when the assembly concentration of ^{F}HBC is higher (Figure 5). Nevertheless, when the concentration of ^{F}HBC is as low as 0.25 mg mL^{-1}, SWNTs with outer and inner diameters of approximately 18 and 12 nm, respectively, can be obtained exclusively (Figure 5a,c). Notably, however, TEM analysis indicated that, at this low concentration of ^{F}HBC, some portions of the SWNTs are wrapped by a nanocoil with an outer diameter of approximately 26 nm (Figure 5d). Such a "coil-on-SWNT" structure was also visualized by SEM microscopy (Figure S8). When the concentration of ^{F}HBC was increased from 0.25 to 0.5 mg mL^{-1} (Figure 5b), double-walled nanotubes (DWNTs) with outer and inner diameters of approximately 26 and 14 nm, respectively, became the predominant form (Figure 5e). At the same time, DWNTs wrapped by a nanocoil (Figure 5f) started to emerge, along with a limited number of MWNTs (Figure 5g). In addition, the nanocoil pitch on the SWNTs appeared to be rather uniform at approximately 40 nm, whereas those on the DWNTs and MWNTs were non-uniform because of their lower morphological integrity.[10] As reported already,[5] coiled tapes are precursors for the HBC nanotubes (Figure 1c).

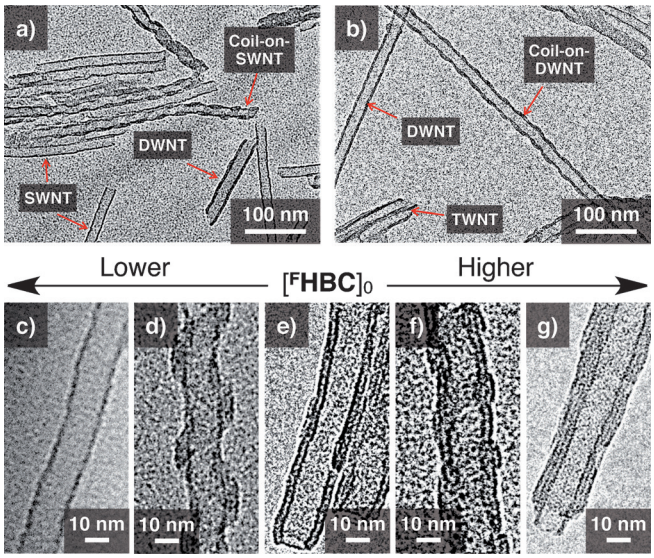

Figure 5. Concentration-dependent morphological changes: a,b) TEM images of an air-dried CH_2Cl_2 suspension of ^{F}HBC at 0.25 and 0.5 mg mL^{-1}. Magnified TEM images of c) a single-walled nanotube (SWNT), d) a coil-on-SWNT, e) a double-walled nanotube (DWNT), f) a coil-on-DWNT, and g) a multi-walled nanotube (MWNT), samples selected from (a) and (b).

Therefore, the "coil-on-tube" structures observed in Figure 5 are possible intermediates for the multiplication of the nanotubular wall. This means that the nanotube undergoes a stepwise radial increase in its number of walls, where the outermost wall may serve as a template for the successive nucleation to initiate the growth of the next outer wall (Figure 2, right). This self-assembling system provides an extraordinary example, where an intermediate involved in each step for constructing a structural hierarchy is clearly observed (Figure 5).[11] We were keen to observe coil-on-tube intermediates in the self-assembly of ^{F}HBC*, since we designed this chiral monomer for investigating how its chiral centers affect the helical sense of the intermediates.[12] However, to our regret, no coil-on-tube intermediates but complete MWNTs were solely observed.

In conclusion, our rational strategy of using perfluoroalkyl segments as solvophilic and solvophobic handles allows for the selective formation of SWNTs and MWNTs from newly designed ^{F}HBC and ^{F}HBC*. Equally important, through careful observation of the electron micrographs, we successfully observed the presence of "coil-on-tube" intermediates for multiplication of the nanotubular wall. This mechanism suggests an interesting possibility that functional MWNTs composed of multiple different walls can be tailored by post-treatment with different HBC derivatives.

Acknowledgements

This work was supported by the Japan Society for the Promotion of Science (JSPS) through its Grant-in-Aid for Specially Promoted Research (25000005) on "Physically Perturbed Assembly for Tailoring High-Performance Soft Materials with Controlled Macroscopic Structural Anisotropy".

Keywords: electron microscopy · helical structures · nanostructures · nanotube · self-assembly

How to cite: *Angew. Chem. Int. Ed.* **2015**, *54*, 11168–11172
Angew. Chem. **2015**, *127*, 11320–11324

[1] a) S. Iijima, *Nature* **1991**, *354*, 56–58; b) P. M. Ajayan, *Chem. Rev.* **1999**, *99*, 1787–1799; c) C. N. R. Rao, B. C. Satishkumar, A. Govindaraj, M. Nath, *ChemPhysChem* **2001**, *2*, 78–105.

[2] a) T. W. Ebbesen, P. M. Ajayan, *Nature* **1992**, *358*, 220–222; b) A. Thess, R. Lee, P. Nikolaev, H. Dai, P. Petit, J. Robert, C. Xu, Y. H. Lee, S. G. Kim, A. G. Rinzler, D. T. Colbert, G. E. Scuseria, D. Tománek, J. E. Fischer, R. E. Smalley, *Science* **1996**, *273*, 483–487; c) C. Journet, W. K. Maser, P. Bernier, A. Loiseau, M. Lamy de La Chapelle, S. Lefrant, P. Deniard, R. Leek, J. E. Fischer, *Nature* **1997**, *388*, 756–758.

[3] a) J.-H. Fuhrhop, W. Helfrich, *Chem. Rev.* **1993**, *93*, 1565–1582; b) T. Shimizu, M. Masuda, H. Minamikawa, *Chem. Rev.* **2005**, *105*, 1401–1443; c) X. Gao, H. Matsui, *Adv. Mater.* **2005**, *17*, 2037–2050; d) H. Yui, H. Minamikawa, R. Danev, K. Nagayama, S. Kamiya, T. Shimizu, *Langmuir* **2008**, *24*, 709–713; e) T. Aida, E. W. Meijer, S. I. Stupp, *Science* **2012**, *335*, 813–817; f) S. S. Babu, S. Prasanthkumar, A. Ajayaghosh, *Angew. Chem. Int. Ed.* **2012**, *51*, 1766–1776; *Angew. Chem.* **2012**, *124*, 1800–1810; g) T. G. Barclay, K. Constantopoulos, J. G. Matisons, *Chem. Rev.* **2014**, *114*, 10217–10291; h) S. S. Babu, V. K. Praveen, A. Ajayaghosh, *Chem. Rev.* **2014**, *114*, 1973–2129.

[4] a) M. S. Spector, K. R. K. Easwaran, G. Jyothi, J. V. Selinger, A. Singh, J. M. Schnur, *Proc. Natl. Acad. Sci. USA* **1996**, *93*, 12943–12946; b) T. Imae, K. Funayama, M. P. Krafft, F. Giulieri, T. Tada, T. Matsumoto, *J. Colloid Interface Sci.* **1999**, *212*, 330–337; c) H. von Berlepsch, C. Böttcher, A. Ouart, M. Regenbrecht, S. Akari, U. Keiderling, H. Schnablegger, S. Dähne, S. Kirstein, *Langmuir* **2000**, *16*, 5908–5916; d) G. John, M. Masuda, Y. Okada, K. Yase, T. Shimizu, *Adv. Mater.* **2001**, *13*, 715–718; e) Z. Wang, C. J. Medforth, J. A. Shelnutt, *J. Am. Chem. Soc.* **2004**, *126*, 15954–15955; f) A. Brizard, C. Aimé, T. Labrot, I. Huc, D. Berthier, F. Artzner, B. Desbat, R. Oda, *J. Am. Chem. Soc.* **2007**, *129*, 3754–3762; g) T. Shimizu, *Bull. Chem. Soc. Jpn.* **2008**, *81*, 1554–1566; h) W. Zhang, W. Jin, T. Fukushima, N. Ishii, T. Aida, *Angew. Chem. Int. Ed.* **2009**, *48*, 4747–4750; *Angew. Chem.* **2009**, *121*, 4841–4844; i) H. Shao, M. Gao, S. H. Kim, C. P. Jaroniec, J. R. Parquette, *Chem. Eur. J.* **2011**, *17*, 12882–12885; j) D. M. Eisele, C. W. Cone, E. A. Bloemsma, S. M. Vlaming, C. G. F. van der Kwaak, R. J. Silbey, M. G. Bawendi, J. Knoester, J. P. Rabe, D. A. Vanden Bout, *Nat. Chem.* **2012**, *4*, 655–662; k) T. G. Barclay, K. Constantopoulos, W. Zhang, M. Fujiki, J. G. Matisons, *Langmuir* **2012**, *28*, 14172–14179; l) W. Liang, S. He, J. Fang, *Langmuir* **2014**, *30*, 805–811; m) F. Rodler, B. Schade, C. M. Jäger, S. Backes, F. Hampel, C. Böttcher, T. Clark, A. Hirsch, *J. Am. Chem. Soc.* **2015**, *137*, 3308–3317.

[5] J. P. Hill, W. Jin, A. Kosaka, T. Fukushima, H. Ichihara, T. Shimomura, K. Ito, T. Hashizume, N. Ishii, T. Aida, *Science* **2004**, *304*, 1481–1483.

[6] W. Jin, Y. Yamamoto, T. Fukushima, N. Ishii, J. Kim, K. Kato, M. Takata, T. Aida, *J. Am. Chem. Soc.* **2008**, *130*, 9434–9440.

[7] *Handbook of Fluorous Chemistry* (Eds.: J. A. Gladysz, D. P. Curran, I. T. Horváth), Wiley-VCH, Weinheim, **2005**.

[8] See Supporting Information.

[9] a) W. Li, A. Amirfazli, *Adv. Mater.* **2007**, *19*, 3421–3422; b) S. Wang, L. Jiang, *Adv. Mater.* **2007**, *19*, 3423–3424.

[10] a) Y.-A. Lin, Y.-C. Ou, A. G. Cheetam, H. Cui, *ACS Macro Lett.* **2013**, *2*, 1088 – 1094; b) Y.-A. Lin, A. G. Cheetam, P. Zhang, Y.-C. Ou, Y. Li, G. Liu, D. Hermida-Merino, I. W. Hamley, H. Cui, *ACS Nano* **2014**, *8*, 12690 – 12700.

[11] X. Zhang, D. Görl, V. Stepanenko, F. Würthner, *Angew. Chem. Int. Ed.* **2014**, *53*, 1270 – 1274; *Angew. Chem.* **2014**, *126*, 1294 – 1298.

[12] a) W. Jin, T. Fukushima, M. Niki, A. Kosaka, N. Ishii, T. Aida, *Proc. Natl. Acad. Sci. USA* **2005**, *102*, 10801 – 10806; b) T. Yamamoto, T. Fukushima, Y. Yamamoto, A. Kosaka, W. Jin, N. Ishii, T. Aida, *J. Am. Chem. Soc.* **2006**, *128*, 14337 – 14340; c) W. Zhang, W. Jin, T. Fukushima, N. Ishii, T. Aida, *J. Am. Chem. Soc.* **2013**, *135*, 114 – 117.

Received: June 24, 2015
Published online: August 12, 2015

